

# Multigrid Simulation for High-Frequency Solutions of the Helmholtz Problem

Seongjai Kim\* and Soohyun Kim†

## Abstract

The Helmholtz problem is hard to solve in heterogeneous media, in particular, when the wave number is real and large. The problem is neither coercive nor Hermitian symmetric. The article is concerned with the  $V$ -cycle multigrid (MG) method for high-frequency solutions of the Helmholtz problem. Since we need to choose at least 10-12 grid points per wavelength for the solution stability, the coarse grid problem is still huge and occupies most of the computation time. To solve the coarse grid problem efficiently, a nonoverlapping domain decomposition method is adopted without introducing another coarser subspace correction. Various numerical experiments have shown that the resulting MG method converges, independently on the grid size and the wave number, when the number of smoothing iterations is not too large and the coarse grid solution captures characteristics of the physical problem.

**Key words.** Helmholtz problem, wave number, attenuation, dispersion, quality factor, multigrid method, domain decomposition method.

**AMS subject classifications.** 65N55, 65F10

---

\*Department of Mathematics, University of Kentucky, Lexington, Kentucky 40506-0027 USA  
Email: skim@ms.uky.edu. He is supported in part by the Summer Faculty Research Fellowship 2000, University of Kentucky Research Foundation.

†Department of Mathematics, Ajou University, 5 Wonchon-Dong, Paldal-Gu, Suwon 442-749, South Korea  
Email: sweete@madang.ajou.ac.kr. Her research is carried out under a partial support from a Brain Korea 21 Project, South Korea.

## 1. Introduction

Let  $\Omega \subset \mathbb{R}^2$  be a rectangular domain with its boundary  $\Gamma = \partial\Omega$ . Consider the following complex-valued Helmholtz problem

$$\begin{aligned} \text{(a)} \quad & -\Delta u - K^2(\mathbf{x})u = S(\mathbf{x}), \quad \mathbf{x} \in \Omega, \\ \text{(b)} \quad & \frac{\partial u}{\partial \nu} + i\alpha(\mathbf{x})u = 0, \quad \mathbf{x} \in \Gamma, \end{aligned} \tag{1.1}$$

where  $i$  is the imaginary unit,  $\nu$  is the unit outward normal from  $\Gamma$ ,  $S$  denotes the source, and the coefficients  $K(\mathbf{x})$  and  $\alpha(\mathbf{x})$  satisfy

$$\begin{aligned} K^2 &= p^2 - iq^2, \quad 0 < p_0 \leq p(\mathbf{x}) \leq p_1 < \infty, \quad 0 \leq q_0 \leq q(\mathbf{x}) \leq q_1 < \infty, \\ \alpha &= \alpha_r - i\alpha_i, \quad \alpha_r > 0, \quad \alpha_i \geq 0, \end{aligned} \tag{1.2}$$

and are sufficiently regular that the existence and uniqueness of a solution of (1.1) lying in  $H^1(\Omega)$  are assured for reasonable sources  $S$ . The coefficient  $\alpha$  is assumed to be properly chosen such that (1.1.b) represents the first-order absorbing boundary condition that allows normally incident waves to pass out of  $\Omega$  transparently. Problem (1.1) models the propagation of time-harmonic waves such as polarized electromagnetic waves and acoustic waves.

When the medium is *barely-attenuative*, i.e.,

$$0 \leq q \ll p, \tag{1.3}$$

the problem (1.1) is hard to solve numerically. In addition to having a complex-valued solution, it is neither Hermitian-symmetric nor coercive, and the algebraic system is not diagonally dominant at all and its Hermitian part is singular. As a consequence, most standard iterative algorithms either fail to converge or converge so slowly to be impractical.

In this article, we consider a multigrid (MG) method for high-frequency solutions of the Helmholtz problem (1.1)-(1.3). Since stability for second-order methods requires to choose at least 10-12 grid points per wavelength, the coarse grid problem is still large for high frequency applications. (The wavelength is defined as  $2\pi/p$ .) To solve the coarse grid problem efficiently, we adopt a domain decomposition (DD) method which is neither overlapping nor incorporating another coarser grid, but accelerated by the artificial damping iteration (ARTDI) and a parameterized Robin interface condition [21].

Concerning other iterative numerical solvers for solving (1.1), we refer to Bayliss *et al.* [1] and Freund [15] for the Krylov subspace algorithms, and Douglas *et al.* [12] for the ADI method. Després [10] studied a DD method on a differential, rather than

a discrete, level and Kim [20, 21, 22, 25] analyzed nonoverlapping DD methods for solving (1.1) by finite difference (FD) and finite element (FE) methods. DD methods incorporating overlapping subdomains and GMRES accelerations have been studied by Widlund and Keyes and their colleagues [9, 32].

An outline of the article is as follows. In the next section, we review various issues in solving the Helmholtz problem: the oscillatory feature of the solution, attenuation and quality factor, and accuracy analysis for the numerical solution. In §3, we present the  $V$ -cycle MG method where the smoothing is performed by the Gauss-Seidel method and the coarse grid problem is solved by a DD method. §4 discusses in detail the coarse grid problem solver, a block-Jacobi-type nonoverlapping DD algorithm accelerated by the ARTDI. Various interesting efficiency issues are considered in the same section. In §5, we present the numerical results to demonstrate efficiency and difficulties of the MG method. It has been numerically verified that the MG method converges independently on the mesh size and the wave number, when the coarse grid problem is fine enough. In §6, we discuss some efficiency issues for the method and future work. The last section concludes our experiments and findings.

## 2. Preliminaries

In this section, we will review physical phenomena such as *attenuation* and *dispersion* and consider difficulties arising in numerical treatments of the barely-attenuative Helmholtz problem (1.1)-(1.3).

### 2.1. Wave number and quality factor

In a class of Geophysical applications of seismic/acoustic waves, the *wave number* is given [4, 26, 28]

$$K(\mathbf{x}) = \frac{\omega}{v(\mathbf{x})}, \quad (2.1)$$

where  $\omega(= 2\pi f)$  is the angular frequency,  $f$  is the frequency, and the complex-valued wave velocity is set as

$$v(\mathbf{x}) = v_0(\mathbf{x})(i\omega)^{\gamma(\mathbf{x})}, \quad \gamma(\mathbf{x}) = \frac{1}{\pi} \tan^{-1} \left( \frac{1}{Q(\mathbf{x})} \right). \quad (2.2)$$

Here  $Q > 0$  is called the *quality factor*; the larger it is, the less attenuative the wave is. The quality factor is known to be between 50 and 300 in most earth media. For a large  $Q$ , we can easily verify

$$\gamma(\mathbf{x}) \approx \frac{1}{\pi Q(\mathbf{x})} \quad \text{and} \quad Q(\mathbf{x}) \approx \frac{p^2(\mathbf{x})}{q^2(\mathbf{x})},$$

where  $K^2(\mathbf{x}) = \omega^2/v^2(\mathbf{x}) = p^2(\mathbf{x}) - iq^2(\mathbf{x})$ . (Set  $Q = \infty$  for  $q = 0$ .)

The quantity  $Q$  is often assumed to be frequency-independent (non-dispersive) and of the following physical interpretation: after the wave travels  $Q$  wavelengths, its magnitude decreases approximately by the factor of  $e^{-\pi}$ , compared with the nonattenuative wave ( $Q = \infty$ ) [4]. It has been numerically verified [25] that the damping coefficient  $q$  affects the wave magnitude *only*, i.e. there is no apparent phase change caused by  $q$ . Such a physical interpretation and numerical verification have motivated the introduction of ARTDI to accelerate the convergence speed of the DD method, the solver for the coarse grid problem, to be presented in §4.

For ocean acoustics, the wave velocity is often assumed to be real, i.e.,

$$K(\mathbf{x}) = \frac{\omega}{v_0(\mathbf{x})}, \quad v(\mathbf{x}) \in \mathbb{R}. \quad (2.3)$$

(For earth media of interests,  $v_0(\mathbf{x})$  has its values between 1.5 Km/s and 4.5 Km/s.) For the electromagnetic waves in homogeneous conducting media,

$$K^2 = \mu\varepsilon\omega^2 - i\mu\sigma\omega, \quad (2.4)$$

where  $\varepsilon$  is the dielectric permittivity,  $\mu$  denotes the magnetic permeability, and  $\sigma$  is the electric conductivity. Note that  $\mu\varepsilon\omega^2 \ll \mu\sigma\omega$  for earth media at frequencies less than  $f = 10^5$  Hz [17]. For most discretization methods, the resulting algebraic system is therefore diagonally dominant and of the form

$$A\mathbf{u} = (P + iR)\mathbf{u} = \mathbf{b}, \quad (2.5)$$

where  $P$  and  $R$  are symmetric with  $R$  being positive definite. Thus the polarized electromagnetic waves having the wave number (2.4) are much easier to simulate than acoustic waves of real-valued wave numbers (2.3). It should be noticed that the existence of a convergent nonsymmetric Krylov subspace algorithm for (2.5) is equivalent to the positive definiteness of  $R$  [14, 18].

## 2.2. Numerical accuracy and iterative methods

For the central second-order FD method or the linear FE method of grid size  $h$ , it has been known [2, 9, 21] that the truncation error is

$$\mathcal{O}(p^3 h^2). \quad (2.6)$$

As a result, the number of points per wavelength has to increase as the wave number grows to maintain a given accuracy. For small or moderate wave numbers  $K$  (or  $p$ ), the grid size  $h$  can be chosen such that

$$ph \leq 1/2 \sim 1/4. \quad (2.7)$$

This choice of  $h$  is the same as choosing at least 12 to 25 grid points per wavelength, and it is often required for accuracy reasons [9, 12, 21, 32, 34].

For iterative algorithms, a coarse grid solution can be used to obtain a better initial guess or to accelerate the convergence. Such an idea has been widely studied in terms of MG methods where one uses a collection of successive coarser meshes [5, 16, 30]. There are two steps in MG methods: coarse grid correction and smoothing. In the coarse grid correction the low and medium frequency components of the error (corresponding to small and medium eigenvalues) are significantly reduced, while the smoothing step reduces the high frequency components of the error. This, roughly speaking, is why the MG method is efficient for solving certain coercive elliptic problems; it is one of most tempting algorithms for the Helmholtz problem.

There exist difficulties in the application of MG methods to the Helmholtz problem. One can find a difficulty in the smoothing step, due to the lack of convergent relaxation algorithms. None of standard relaxation algorithms are convergent for the problem. One can encounter another difficulty in the coarse grid correction. The huge, poorly-conditioned, non-Hermitian coarse grid problem should be solved without introducing another coarser mesh. Obviously, it is quite expensive!

### 2.3. Difficulties in the coarse grid solve

In this subsection, we will discuss difficulties in solving the coarse grid problem of MG methods for the Helmholtz problem. Let  $\Omega = (0, 1)^2$ ,  $\mathbf{x} = (x, y) \in \Omega$ , and

$$p(x, y) = \frac{\omega}{v(x, y)}, \quad q \equiv 0;$$

select two real-valued velocities as

$$\begin{aligned} v_1(x, y) &\equiv 2, \\ v_2(x, y) &= 1 + x^3 + 1.5y. \end{aligned} \tag{2.8}$$

We choose either a point source, i.e.,  $S(\mathbf{x}) = \delta(\mathbf{x} - \mathbf{x}_0)$  for some  $\mathbf{x}_0 \in \Omega$ , or a distributed source. Consider

$$u(x, y) = \phi(x)\phi(y), \quad \phi(x) = e^{i\omega(x-1)} + e^{-i\omega x} - 2. \tag{2.9}$$

Then, a distributed source  $S(x, y)$  can be chosen such that  $u$  in (2.9) satisfies (1.1.a) exactly. (Note that  $u$  satisfies the boundary condition (1.1.b) when  $\alpha = \omega$ .)

The wavelength is by definition  $v/f (= 2\pi/p)$ . Consider the uniform mesh of grid size  $h$ . Then, the *grid frequency* (GF) can be defined as the average number of grid points per wavelength:

$$G_f = \frac{\hat{v}}{fh}, \tag{2.10}$$

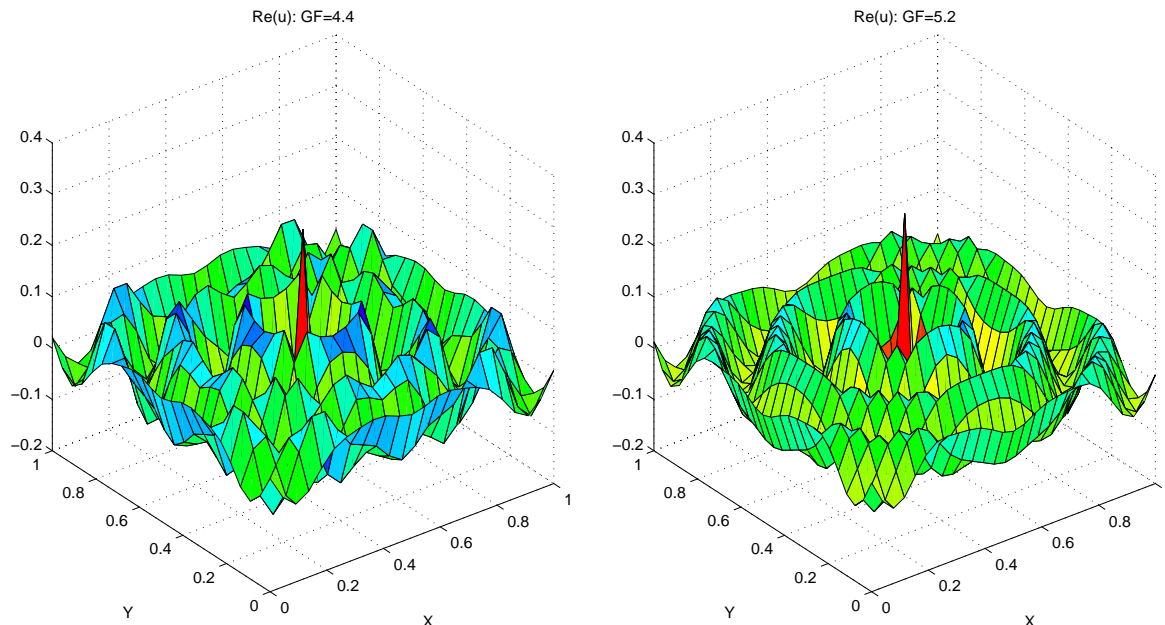


Figure 1: The real parts of the solutions for the grid frequencies 4.4 (left) and 5.2 (right). Set  $v = v_1$  and  $f = 10$  and the point source is located at  $(0.5, 0.5)$ .

Table 1: The grid frequencies for stability. The source  $S$  is set for the solution (2.9) to satisfy (1.1.a) exactly.

	$v = v_1$	$v = v_2$
$f = 5$	5.6	7.2
$f = 10$	6.4	9.0
$f = 20$	8.4	11.5

where  $\hat{v}$  is an average of the velocity over the region under consideration. The stability requires  $G_f$  to be sufficiently large; we will see later in the paper that  $G_f$  must be at least 10-12.

Figure 1 shows the real parts of the solutions for two different grid frequencies, when  $v = v_1$ ,  $f = 10$ , and a point source is located at the center of the domain, i.e.,  $S(\mathbf{x}) = \delta(\mathbf{x} - \mathbf{x}_0)$ ,  $\mathbf{x}_0 = (0.5, 0.5)$ . The algebraic systems are solved directly by an  $LU$ -factorization with partial pivoting. The solution deteriorates rapidly as  $G_f$  decreases below five, which indicates instability. Therefore one can say that the GF must be at least five for stability.

Table 1 presents the GFs for stable solutions for various pairs of velocities  $v$  and frequencies  $f$ . The source  $S$  is set for the solution (2.9) to satisfy (1.1.a) exactly.

It seems that for meaningful numerical solutions, the GF should be at least 6-8 for homogeneous media and at least 10 for general media, even for moderately-high frequency solutions. It should be noticed that the GF for stability increases as the frequency grows; see also (2.6).

Here appears the major difficulty when MG methods are to be applied to the high-frequency Helmholtz problem. Realistic applications often require numerical solutions of 10 to 50 wavelengths. For the simulation of 20 wavelengths, for example, if the GF is expected to be 10 for stability, we need to choose at least 200 grid points in each direction for the coarse grid problem; the solution on *coarser* meshes will not be able to capture characteristics of the physical problem. Efficiency of a MG method depends strongly on that of the coarse grid solver.

### 3. The multigrid method

Let the Helmholtz problem (1.1) be discretized by a approximation scheme on a finite dimensional space  $V^h$ , where  $h$  is the grid size. Then the resulting algebraic system can be written as

$$A^h \mathbf{u}^h = \mathbf{b}^h, \quad (3.1)$$

where  $A^h$  is a complex-valued, non-Hermitian, square matrix,  $\mathbf{u}^h$  is the unknown vector, and  $\mathbf{b}^h$  denotes the source vector.

Let  $h_1 \geq h$  be the element size for a coarser grid mesh and  $V^{h_1}$  be the corresponding proper subspace of  $V^h$ . First, consider the following two-grid algorithm:

$$\begin{aligned}
 & \text{Select } \mathbf{u}^{h,0}, \varepsilon; \\
 & \text{Do } m = 0, 1, \dots \\
 & \quad \text{(i) } \mathbf{r}^{h,m} = \mathbf{b}^h - A^h \mathbf{u}^{h,m}; \\
 & \quad \text{(ii) if } \|\mathbf{r}^{h,m}\|_\infty < \varepsilon \|\mathbf{r}^{h,0}\|_\infty, \text{ stop}; \\
 & \quad \text{(iii) solve } A^{h_1} \mathbf{e}^{h_1} = I_h^{h_1}(\mathbf{r}^{h,m}); \\
 & \quad \text{(iv) } \mathbf{u}^{h,m+1/2} = \mathbf{u}^{h,m} + I_{h_1}^h(\mathbf{e}^{h_1}); \\
 & \quad \text{(v) } \mathbf{u}^{h,m+1} = S_m(\mathbf{u}^{h,m+1/2}); \\
 & \text{Enddo}
 \end{aligned} \quad (3.2)$$

Here the operators  $I_h^{h_1}$  and  $I_{h_1}^h$  denote the projection from  $V^h$  to  $V^{h_1}$  and the prolongation from  $V^{h_1}$  to  $V^h$ , respectively, and  $S_m$  is a smoothing operator. We will utilize the Gauss-Seidel (GS) method for the smoothing iteration. The above two-grid algorithm is the simplest case of MG methods. A MG algorithm can be obtained by trying to solve (3.2.iii) in another proper subspace  $V^{h_2} \subset V^{h_1}$  corresponding to another coarser grid mesh,  $h_2 \geq h_1$ .

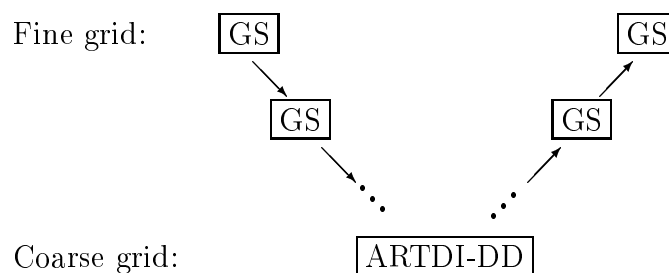


Figure 2: Algorithm overview for the  $V$ -cycle MG method.

Smoothers such as Jacobi and GS methods can expand the low-frequency components of the error, while the smoothers reduce the high-frequency components efficiently. When the coarse grid correction can decrease the low-frequency components of the error by a larger factor than the smoother's expansion, the MG method would converge. A convergence analysis based on the mathematical framework exploited by Bramble and his colleagues [7, 8] will appear elsewhere [24].

To solve the coarse grid problem which is still large and poorly-conditioned, we would like to employ a DD method. It is a common practice that DD methods for solving coercive problems have been accelerated by a coarse subspace correction and overlapping subdomains [13, 27, 36]. However, in our case, any meaningful coarser mesh may not be introduced to accelerate the DD method. Also it is hard to see *physical* reasons for the incorporation of overlapping subdomains to improve the convergence speed of the DD method, due to the highly oscillatory characteristics of the solution. (With overlapping subdomains, one can deal with the Robin interface condition more flexibly.) That is, the conventional acceleration techniques are hardly applicable to the DD method for the Helmholtz problem.

One of authors has studied a nonoverlapping DD method which does not incorporate the coarse subspace correction, but is accelerated by the so-called *artificial damping iteration* (ARTDI) and a parameterized Robin interface condition [21, 25]. The resulting algorithm, *ARTDI-DD*, has been numerically verified that its convergence rate is independent on the mesh size  $h$ . (The convergence rate is, and must be, dependent on the subdomain size, because there is no global correction involved; see [13].) We have found ARTDI-DD is particularly appropriate for the solution of the coarse grid problem. Figure 2 overviews the resulting MG method.

## 4. The coarse grid problem solver: DD method

The coarse grid problem is large and poorly-conditioned. It is hard to solve either by a direct method due to its problem size or by an iterative algorithm because of its large condition number. In this context, DD methods are attractive for such a large poorly-conditioned problem; DD methods combine iterative methods at the interface level and direct algorithms at the subdomain level.

In this section, we first present a FD revision of the nonoverlapping DD algorithm that was suggested and analyzed (in variational formulation) by one of the authors [21]. Then, we try to point out interesting efficiency issues for the algorithm with numerical verifications.

### 4.1. Decomposition of the problem

Assume the domain  $\Omega$  is rectangular, for simplicity. Let  $\{\Omega_j, j = 1, 2, \dots, M\}$  be a partition of  $\Omega$ :

$$\begin{aligned} \bar{\Omega} &= \cup_{j=1}^M \bar{\Omega}_j; & \Omega_j \cap \Omega_k &= \emptyset, \quad j \neq k; \\ \Gamma_j &= \Gamma \cap \partial\Omega_j; & \Gamma_{jk} &= \Gamma_{kj} = \partial\Omega_j \cap \partial\Omega_k. \end{aligned}$$

Also we assume that  $\Omega_j$  are rectangles. Decompose problem (1.1) over the partition:

$$\begin{aligned} \text{(a)} \quad & -\Delta u_j - K^2 u_j = S(\mathbf{x}), & \mathbf{x} \in \Omega_j, \\ \text{(b)} \quad & \frac{\partial u_j}{\partial \nu_j} + i\alpha u_j = 0, & \mathbf{x} \in \Gamma_j, \\ \text{(c)} \quad & \frac{\partial u_j}{\partial \nu_j} + i\beta u_j = -\frac{\partial u_k}{\partial \nu_k} + i\beta u_k, & \mathbf{x} \in \Gamma_{jk}, \end{aligned} \tag{4.1}$$

where  $\beta$ ,  $\text{Re}(\beta) > 0$ , is a relaxation parameter. The positivity of  $\text{Re}(\beta)$  is required for the well-posedness of the subproblems in (4.1) restricted to a subdomain. Equation (4.1.c) is a parameterized *Robin interface condition* (RIC) and can be equivalently rewritten as the following consistency conditions

$$u_j = u_k, \quad \frac{\partial u_j}{\partial \nu_j} = -\frac{\partial u_k}{\partial \nu_k}, \quad \mathbf{x} \in \Gamma_{jk}. \tag{4.2}$$

The basic idea of a DD iterative method is to localize the computations to smaller subdomain problems. It is feasible to localize to each  $\Omega_j$  by evaluating the quantities in (4.1) related to each  $\Omega_j$  at the new iterate level and those in (4.1) related to neighboring subdomains  $\Omega_k$  at the old level. The iterative algorithm in the differential

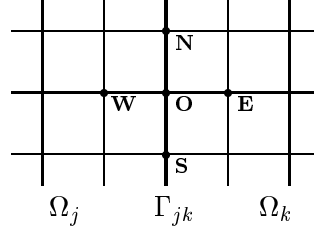


Figure 3: The five point stencil at a grid point on the interface  $\Gamma_{jk}$ .

case can be defined as follows: Given  $\{u_j^0\}$ , find  $\{u_j^n\}$ ,  $n \geq 1$ , by solving

$$\begin{aligned}
 \text{(a)} \quad & -\Delta u_j^n - K^2 u_j^n = S(\mathbf{x}), & \mathbf{x} \in \Omega_j, \\
 \text{(b)} \quad & \frac{\partial u_j^n}{\partial \nu_j} + i\alpha u_j^n = 0, & \mathbf{x} \in \Gamma_j, \\
 \text{(c)} \quad & \frac{\partial u_j^n}{\partial \nu_j} + i\beta u_j^n = -\frac{\partial u_k^{n-1}}{\partial \nu_k} + i\beta u_k^{n-1}, & \mathbf{x} \in \Gamma_{jk}.
 \end{aligned} \tag{4.3}$$

For the solution in homogeneous media ( $K = \alpha = \beta \equiv \omega$ ), Després [10, 11] applied the arguments in Lions [29] to analyze the convergence of algorithm (4.3) on a differential level. Kim [20, 21] studied the algorithm for the FD and FE solutions of the Helmholtz problem in general media.

#### 4.2. The DD method on a discrete level

There is a technical difficulty in the use of RIC for nonoverlapping DD methods incorporating FD methods or conforming FE methods. RIC imposes, on the subdomain interfaces, the continuity of both the discrete solution and its normal flux, while the standard FE methods allow the normal flux to be discontinuous. Therefore, in a discrete DD algorithm, the terms  $\partial u_j^n / \partial \nu_j$  and  $\partial u_k^{n-1} / \partial \nu_k$  in (4.3.c) should be carefully treated. Here the requirement is that the decomposed problem should be equivalent to the original problem, i.e., the limit of the discrete DD iterates (if any) must be the same as the original discrete solution. As a choice, we approximate the normal derivatives by one-sided finite differences.

Let the domain be discretized into uniform cells of edge size  $h_c$  and the subdomain interfaces  $\{\Gamma_{jk}\}$  coincide with parts of grid lines. Let  $\partial_{\mathbf{b},jk} u_j$  and  $\partial_{\mathbf{f},jk} u_j$  be the backward and forward differences for  $\partial u_j / \partial \nu_j$  on  $\Gamma_{jk}$ , respectively. For example, at the nodal point  $\mathbf{o} \in \Gamma_{jk}$  in Figure 3, they are defined as

$$\begin{aligned}
 \partial_{\mathbf{b},jk} u_j(\mathbf{o}) &= (u_j(\mathbf{o}) - u_j(\mathbf{w})) / h_c, & \partial_{\mathbf{f},jk} u_j(\mathbf{o}) &= (u_j(\mathbf{e}) - u_j(\mathbf{o})) / h_c, \\
 \partial_{\mathbf{b},kj} u_k(\mathbf{o}) &= (u_k(\mathbf{o}) - u_k(\mathbf{e})) / h_c, & \partial_{\mathbf{f},kj} u_k(\mathbf{o}) &= (u_k(\mathbf{w}) - u_k(\mathbf{o})) / h_c.
 \end{aligned}$$

(Here we have employed an exterior bordering of the subdomains.) Let  $\Delta_{h_c} u_j$  be the central five-point difference approximation of  $\Delta u_j$  and  $\partial_{\mathbf{c},j} u_j$  be the central difference for  $\partial u_j / \partial \nu_j$  on the boundary  $\Gamma_j$ .

Then the DD iterative algorithm in the FD formulation can be defined as follows: For given  $\{u_j^0\}$ , find  $\{u_j^n\}$ ,  $n \geq 1$ , by recursively solving

$$\begin{aligned} \text{(a)} \quad & -\Delta_{h_c} u_j^n - K^2 u_j^n = S, & \mathbf{x} \in \Omega_j, \\ \text{(b)} \quad & \partial_{\mathbf{c},j} u_j^n + i\alpha u_j^n = 0, & \mathbf{x} \in \Gamma_j, \\ \text{(c)} \quad & \partial_{\mathbf{f},jk} u_j^n + i\beta u_j^n = -\partial_{\mathbf{b},kj} u_k^{n-1} + i\beta u_k^{n-1}, & \mathbf{x} \in \Gamma_{jk}. \end{aligned} \quad (4.4)$$

Note that the *modified* RIC (4.4.c) imposes the continuity of the discrete solution only, when the algorithm converges. Such a modification of the parameterized RIC, the *forward-backward difference matching* (4.4.c), is introduced to enforce equivalence to the original discrete problem. When overlapping subdomains are introduced as in [9, 32], it is more flexible to choose a matching condition.

In the following, we check the equivalence of algorithm (4.4) to the original discrete problem. It suffices to consider the algebraic equations of (4.4) at interface grid points. At the point  $\mathbf{o}$  (in Figure 3), the equation (4.4.a) reads

$$(4 - h_c^2 K_{\mathbf{o}}^2) u_{j,\mathbf{o}}^n - u_{j,\mathbf{E}}^n - u_{j,\mathbf{W}}^n - u_{j,\mathbf{S}}^n - u_{j,\mathbf{N}}^n = h_c^2 S_{\mathbf{o}}, \quad (4.5)$$

where  $u_{j,\mathbf{o}}^n = u_j^n(\mathbf{o})$ , the value of  $u_j^n$  at the point  $\mathbf{o}$ , and the others are similarly defined. The term  $u_{j,\mathbf{E}}^n$  in (4.5) evaluated at a point out of the subdomain  $\Omega_j$  can be substituted by using (4.4.c). Equation (4.4.c) is written as

$$\frac{u_{j,\mathbf{E}}^n - u_{j,\mathbf{o}}^n}{h_c} + i\beta u_{j,\mathbf{o}}^n = \frac{u_{k,\mathbf{E}}^{n-1} - u_{k,\mathbf{o}}^{n-1}}{h_c} + i\beta u_{k,\mathbf{o}}^{n-1},$$

or equivalently

$$u_{j,\mathbf{E}}^n - (1 - i\beta h_c) u_{j,\mathbf{o}}^n = u_{k,\mathbf{E}}^{n-1} - (1 - i\beta h_c) u_{k,\mathbf{o}}^{n-1}. \quad (4.6)$$

Substituting (4.6) into (4.5), we have

$$\begin{aligned} [4 - h_c^2 K_{\mathbf{o}}^2 - (1 - i\beta h_c)] u_{j,\mathbf{o}}^n - u_{j,\mathbf{W}}^n - u_{j,\mathbf{S}}^n - u_{j,\mathbf{N}}^n \\ = h_c^2 S_{\mathbf{o}} + u_{k,\mathbf{E}}^{n-1} - (1 - i\beta h_c) u_{k,\mathbf{o}}^{n-1}. \end{aligned} \quad (4.7)$$

In the same manner, one can treat cross points arising in a box-type decomposition of the domain. When the algorithm converges, the limit would clearly satisfy the original algebraic equation

$$(4 - h_c^2 K_{\mathbf{o}}^2) u_{\mathbf{o}} - u_{\mathbf{E}} - u_{\mathbf{W}} - u_{\mathbf{S}} - u_{\mathbf{N}} = h_c^2 S_{\mathbf{o}},$$

which proves the equivalence of (4.4) to the original discrete problem.

Algorithm (4.4) is applicable to nonuniform meshes with minor changes. One can easily see its convergence by following the arguments in [21] where the analysis is carried out in variational formulation. Let  $\mathcal{A}$  be the iteration matrix of (4.4). Then, its spectral radius can be minimized and bounded as

$$\rho(\mathcal{A}) \leq 1 - C \frac{q_0^4}{p_1^2} h_c^2, \quad (4.8)$$

for some  $C > 0$  independent of  $h_c$  and  $K$ , when the parameter  $\beta = \beta_r - i\beta_i$  is carefully chosen. When  $q_0 = 0$ , we do not know of any convergence analysis of the DD method.

### 4.3. Artificial damping iteration

The convergence of algorithm (4.4) strongly depends on (and is most sensitive to) the damping coefficient  $q$ , as shown in (4.8). As  $q$  becomes smaller, the DD method either converges slowly or fails to converge. To overcome the difficulty, we consider the artificial damping iteration (ARTDI).

Let the coarse grid problem be given as

$$A^{h_c} \mathbf{u}^{h_c} = \mathbf{b}^{h_c}. \quad (4.9)$$

Then, ARTDI is formulated as follows: Select  $\mathbf{u}^{h_c,0}$  and  $d > 0$ ; then find  $\mathbf{u}^{h_c,\ell}$ ,  $\ell \geq 1$ , satisfying

$$(A^{h_c} + idI) \mathbf{u}^{h_c,\ell} = \mathbf{b}^{h_c} + id\mathbf{u}^{h_c,\ell-1}, \quad (4.10)$$

or, equivalently,

$$\begin{aligned} (A^{h_c} + idI) \boldsymbol{\delta}^{\ell-1} &= \mathbf{b}^{h_c} - A^{h_c} \mathbf{u}^{h_c,\ell-1}, \\ \mathbf{u}^{h_c,\ell} &= \mathbf{u}^{h_c,\ell-1} + \boldsymbol{\delta}^{\ell-1}, \end{aligned} \quad (4.11)$$

where  $I$  is the identity matrix.

Since  $d$  corresponds to a positive damping coefficient, one can solve each step of (4.10) easily by utilizing the DD method (4.4). That is, ARTDI and the DD method serve as the outer and inner loops, respectively, for solving (4.9). The inner loop is not necessary to solve completely; we force the inner loop to stop in  $n_*$  iterations.

Then the algorithm *ARTDI-DD* can be formulated as

Select  $\varepsilon_D$ ,  $\eta$ , and  $n_*$  ;  
 Choose the initial value  $\mathbf{u}^{h_c,0} = \{u_j^0\}_{j=1,\dots,M}$  ;  
 Compute  $\|\mathbf{r}^0\|_\infty = \|\mathbf{b}^{h_c} - A^{h_c}\mathbf{u}^{h_c,0}\|_\infty$  ;  
 For  $\ell = 1, 2, \dots$   
    $u_j^{\ell,0} = u_j^{\ell-1}$ ,  $j = 1, \dots, M$  ;  
   Do  $n = 1, \dots, n_*$   
     
$$\begin{cases} -\Delta_{h_c} u_j^{\ell,n} - K^2 u_j^{\ell,n} + i\eta^2 u_j^{\ell,n} = S + i\eta^2 u_j^{\ell-1}, & \mathbf{x} \in \Omega_j, \\ \partial_{\mathbf{c},j} u_j^{\ell,n} + i\alpha u_j^{\ell,n} = 0, & \mathbf{x} \in \Gamma_j, \\ \partial_{\mathbf{r},jk} u_j^{\ell,n} + i\beta u_j^{\ell,n} = -\partial_{\mathbf{b},kj} u_k^{\ell,n-1} + i\beta u_k^{\ell,n-1}, & \mathbf{x} \in \Gamma_{jk}. \end{cases} \quad (4.12)$$
  
   End do  
    $u_j^\ell = u_j^{\ell,n_*}$ ,  $j = 1, \dots, M$  ;  
   if  $\|\mathbf{b}^{h_c} - A^{h_c}\mathbf{u}^{h_c,\ell}\|_\infty \leq \varepsilon_D \|\mathbf{r}^0\|_\infty$ , stop ;  
 End for

For the central FD method, the coefficients  $d$  and  $\eta$  are related as  $d = \eta^2 h_c^2$ . Here we consider an efficient way of choosing parameters  $n_*$  and  $\eta$ . Let the domain in 2D be decomposed into  $M_x$  and  $M_y$  subdomains in  $x$ - and  $y$ -directions, respectively. It has been numerically verified that (4.12) converges fastest (in computation time) with the following choices:

$$n_* = 1 + \left( \frac{M_x + M_y}{4} \sim \frac{M_x + M_y}{5} \right), \quad \eta = \frac{\hat{p}}{3} \sim \frac{\hat{p}}{5}, \quad (4.13)$$

where  $\hat{p}$  is the  $L^2$ -average of  $p$  over the domain; see Table 2 below. For most cases having realistic quality factors, ARTDI-DD (4.12) incorporating (4.13) converges 2-20 times faster than (4.4). Note that in (4.8), the most sensitive component to the convergence rate is  $q^2$ ; in ARTDI-DD,  $(q^2 + \eta^2)$  plays the same role for the inner loop.

#### 4.4. Algebraic interpretation of ARTDI

One can prove the convergence of (4.12) for  $n_*$  sufficiently large, whether the physical damping coefficient  $q$  is zero or not. The convergence analysis is based on the fact that the imaginary parts of eigenvalues of  $A^{h_c}$  are all nonnegative; or, equivalently,  $A^{h_c} - (cI - idI)$  is nonsingular for every  $c \in \mathbb{R}$  and  $d > 0$ .

In this subsection, we algebraically interpret the convergence of (4.10). Let  $\sigma(A^{h_c}) = \{\lambda_j : j = 1, 2, \dots, N\}$  be the spectrum of  $A^{h_c}$  with

$$\operatorname{Re}(\lambda_1) \leq \operatorname{Re}(\lambda_2) \leq \dots \leq \operatorname{Re}(\lambda_N),$$

and  $\{\mathbf{v}_j : j = 1, 2, \dots, N\}$  be the corresponding eigenvectors. Then,

$$-\xi_1^2 \leq \operatorname{Re}(\lambda_j) \leq 8 - \xi_0^2, \quad j = 1, \dots, N, \quad (4.14)$$

where  $\xi_k = p_k h_c$ ,  $k = 0, 1$ . (We will accept  $\operatorname{Im}(\lambda_j) \geq 0$  without proof.)

For problems of small size, the eigenvalues can be easily found with sufficient accuracy using public domain codes such as one available from EISPACK or LAPACK. One can see in practice that  $\operatorname{Im}(\lambda_j) > 0$ ,  $j = 1, \dots, N$ , and the eigenvalues are distinct; we may assume that the eigenvectors are orthonormal. Define

$$\mathbf{e}^\ell = \mathbf{u}^{h_c} - \mathbf{u}^{h_c, \ell},$$

where  $\mathbf{u}^{h_c, \ell}$  is the  $\ell$ -th iterate of (4.10). Then, it follows from (4.9) and (4.10) that

$$(A^{h_c} + idI)\mathbf{e}^\ell = id\mathbf{e}^{\ell-1}. \quad (4.15)$$

Let

$$\mathbf{e}^\ell = \sum_{j=1}^N a_j \mathbf{v}_j, \quad \mathbf{e}^{\ell-1} = \sum_{j=1}^N b_j \mathbf{v}_j.$$

Then (4.15) reads

$$\sum_{j=1}^N (\lambda_j + id) a_j \mathbf{v}_j = \sum_{j=1}^N id b_j \mathbf{v}_j.$$

Multiplying both sides of the above equation by  $\mathbf{v}_j$ , we have

$$a_j = \frac{id}{\lambda_j + id} b_j, \quad j = 1, \dots, N, \quad (4.16)$$

and therefore

$$\|\mathbf{e}^\ell\| \leq \max_{\lambda_j \in \sigma(A^{h_c})} \frac{d}{|\lambda_j + id|} \cdot \|\mathbf{e}^{\ell-1}\| = \frac{d}{|\lambda_{j^*} + id|} \cdot \|\mathbf{e}^{\ell-1}\|, \quad (4.17)$$

where  $\lambda_{j^*}$  is the eigenvalue of  $A^{h_c}$  nearest to  $-id$ . Recall  $\operatorname{Im}(\lambda_j) \geq 0$ ,  $j = 1, \dots, N$ . Since  $A^{h_c}$  has been assumed nonsingular, i.e.,  $0 \notin \sigma(A^{h_c})$ , the inequality (4.17) proves the convergence of ARTDI (4.10).

#### 4.5. Numerical convergence of ARTDI

ARTDI would converge faster as  $d$  decreases; however, solving the corresponding inner loop would become more expensive. A guideline seems necessary to select an efficient artificial damping coefficient  $\eta$ . We have found from various numerical experiments that  $\eta$  can be best chosen for the *artificial quality factor*  $Q_a$  ( $:= \hat{p}^2/\eta^2$ ) to become approximately 10-25. See (4.13). It is numerically verified that when  $Q = \infty$ ,

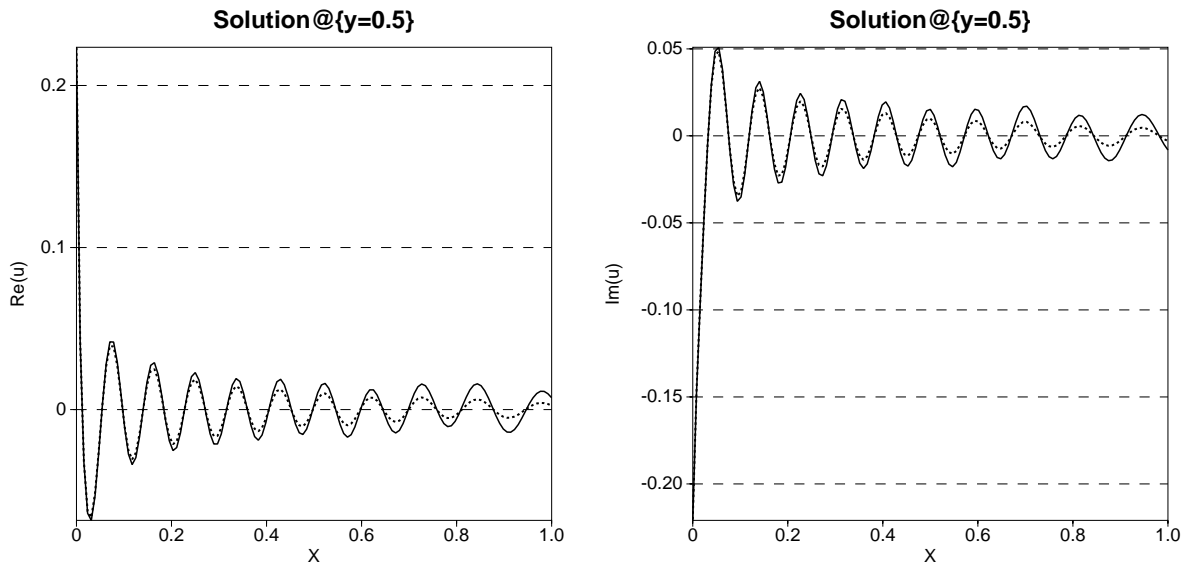


Figure 4: The real (left) and the imaginary (right) parts of the solution on the slice  $\{y = 0.5\}$  for  $f = 20$ ,  $v = v_2$ ,  $q = 0$ , and  $h_c = 1/128$ ; a point source is located at  $(0, 0.5)$ . In each side, the solid curve and the dotted curve correspond respectively to  $\eta = 0$  ( $Q_a = \infty$ ) and  $\eta = 13.6$  ( $Q_a = 20$ ).

$Q_a \approx 20$ , and the inner loop is solved with a sufficient accuracy (i.e.  $n_*$  is large), ARTDI could reduce the  $L^\infty$ -residual error by a digit in two iterations. To see this, let us consider an example. Let  $Q_a = 20$  and  $G_f = 12$ . Then,

$$d = \eta^2 h_c^2 = \frac{\hat{p}^2 h_c^2}{20} = \frac{4\pi^2}{2880} \approx 0.0137.$$

It can be seen from (4.16) that most eigen-components of the error are reduced by at least one order in each iteration of ARTDI, except those having eigenvalues near the origin (i.e.  $|\lambda_j| \leq 0.14$ ).

The rapid convergence of ARTDI can be explained also by the observation that the damped solution  $\mathbf{u}^{h_c,1}$  (the first iterate of (4.10) starting from  $\mathbf{u}^{h_c,0} = 0$ ) is a slight perturbation of the original discrete solution  $\mathbf{u}^{h_c}$ . Figure 4 depicts computed solutions on the line segment  $\{y = 0.5\}$  when  $\Omega = (0, 1)^2$ ,  $f = 20$ ,  $v = v_2$  as given in (2.8),  $q = 0$ ,  $h_c = 1/128$ , and  $S(\mathbf{x}) = \delta(\mathbf{x} - \mathbf{x}_0)$ , where  $\mathbf{x}_0 = (0, 0.5)$ . In each side, the solid curve and the dotted curve correspond respectively to  $\mathbf{u}^{h_c}$  and  $\mathbf{u}^{h_c,1}$  ( $\eta = 13.6$  or  $Q_a = 20$ ). As one can see from the figure, the damped solution  $\mathbf{u}^{h_c,1}$  incorporates no apparent phase error and its amplitude matches well with the original discrete solution near the source and decreases gradually far away from the source.

In Table 2, we present the number of ARTDI iterations ( $\ell$ ) and the elapsed time

Table 2: The number of ARTDI iterations ( $\ell$ ) and the elapsed time (CPU) for ARTDI-DD (4.12) to reduce the  $L^\infty$ -residual by the factor of  $10^{-5}$ , for  $Q_a = 20$  and  $M_x \times M_y = 8 \times 1$ . Set  $f = 20$ ,  $q = 0$ ,  $h_c = 1/128$ , and  $S(\mathbf{x}) = \delta(\mathbf{x} - \mathbf{x}_0)$ , where  $\mathbf{x}_0 = (0, 0.5)$ .

	$n_* = 2$		$n_* = 4$		$n_* = 6$		$n_* = 8$		$n_* = 10$	
	$\ell$	CPU	$\ell$	CPU	$\ell$	CPU	$\ell$	CPU	$\ell$	CPU
$v = v_1$	15	3.3	9	3.9	8	5.1	7	5.8	7	7.2
$v = v_2$	15	3.4	10	4.3	8	5.1	8	6.5	8	8.1

Table 3: The total number of DD iterations ( $N_{DD}$ ) and CPU, for (4.12). Set  $q = 0$ ,  $v = v_2$ , and a point source at  $\mathbf{x}_0 = (0, 0.5)$ .

$M_x \times M_y$	$h = 1/256$				$h = 1/512$			
	$f = 10$		$f = 20$		$f = 10$		$f = 20$	
	$N_{DD}$	CPU	$N_{DD}$	CPU	$N_{DD}$	CPU	$N_{DD}$	CPU
$16 \times 1$	56	22.5	64	25.1	56	163.8	64	180.0
$16 \times 2$	60	23.9	64	25.0	64	180.3	64	180.2
$16 \times 4$	75	28.7	85	32.2	65	183.2	80	219.8
$16 \times 8$	75	28.7	90	34.3	75	207.8	85	231.0
$16 \times 16$	98	37.8	119	44.5	98	263.9	112	298.2

(CPU) for ARTDI-DD (4.12) to reduce the  $L^\infty$ -residual by the factor of  $10^{-5}$  ( $\varepsilon_D = 10^{-5}$ ), for  $Q_a = 20$  and  $M_x \times M_y = 8 \times 1$ . The computation is carried out on a 400 MHz laptop having 192M memory and a Linux operating system; CPU is the user time measured in second. We set  $f = 20$ ,  $q = 0$ ,  $h_c = 1/128$ , and  $S(\mathbf{x}) = \delta(\mathbf{x} - \mathbf{x}_0)$ , where  $\mathbf{x}_0 = (0, 0.5)$ . The overall convergence rate of ARTDI is not altered much, when the inner loop is solved with  $n_* \geq 6$ . However, the total number of DD iterations (and therefore, the computation time) is minimized when  $n_* = 2$ ; see (4.13).

Table 3 shows the total number of DD iterations ( $N_{DD}$ ) and CPU for the algorithm (4.12) with the tolerance  $\varepsilon_D = 10^{-5}$ . We set  $q = 0$ ,  $v = v_2$ , and  $S(\mathbf{x}) = \delta(\mathbf{x} - \mathbf{x}_0)$ , where  $\mathbf{x}_0 = (0, 0.5)$ . For the computation, we choose the parameters

$$n_* = 1 + \frac{M_x + M_y}{5} \quad \text{and} \quad \eta = \frac{\hat{p}}{3.5}.$$

The convergence rate is independent on the grid size  $h$  and slightly dependent on the wave number  $K$ . The total number of DD iterations approximately becomes

$$N_{DD} \approx 3.5 \cdot (M_x + M_y),$$

for the algorithm to reduce the  $L^\infty$ -residual by five digits.

*Remark.* For the Helmholtz problem, Widlund and Keyes and their colleagues [9, 32] studied DD methods accelerated by a coarse grid solution, subdomain overlapping, and/or Krylov subspace methods (e.g. GMRES [33]). These conventional acceleration techniques should be carefully applied to achieve a convergence of the resulting DD method. On the other hand, our DD method accelerated by ARTDI converges with a great efficiency, even for problems having small grid frequencies. For example, when  $h = 1/256$ ,  $f = 50$  ( $5.1 \leq G_f \leq 17.9$ ), and the other parameters are set the same as in Table 3, the DD method converges in 96 (36.4 sec) and 189 (71.1 sec) iterations respectively for  $16 \times 1$  and  $16 \times 16$  subdomains. (The computed solution hardly shows wave characteristics, though.)

*Remark.* One may carry out the inner loop (the DD iteration) with an application of a red-black ordering or the block Gauss-Seidel method, to enjoy an improved efficiency. We will not try to address issues in the direction.

## 5. Numerical experiments with the $V$ -cycle MG method

The  $V$ -cycle MG algorithm is implemented with the coarse grid problem being solved by ARTDI-DD (4.12); we apply the smoothing operator ( $\gamma$  Gauss-Seidel iterations) in each of projection and prolongation steps. The main/driver routines are written in C++ and the core computation routines are in F77. The computation is carried out on the same machine as before: a 400 MHz laptop. The elapsed time (CPU) is the user time measured in second.

Choose  $\Omega = (0, 1)^2$ . Besides the velocities in (2.8), we consider

$$\begin{aligned} v_3(x, y) &= 1.6 + |\sin(3\pi x) \cdot \cos(4\pi y)|, \\ v_4(x, y) &= \begin{cases} 2, & \text{if } x \leq 0.5, \\ 2 + \sin(5\pi xy), & \text{else.} \end{cases} \end{aligned} \quad (5.1)$$

(The velocities are chosen such that the  $L^2$ -average is about 2.) A point source is located at the center of the domain, i.e.,  $S(\mathbf{x}) = \delta(\mathbf{x} - \mathbf{x}_0)$ , where  $\mathbf{x}_0 = (0.5, 0.5)$ .

The MG iteration begins with the zero initial value ( $\mathbf{u}^{h,0} = 0$ ) and ends when the  $L^\infty$ -residual is reduced by the factor of  $10^{-5}$ , i.e.,

$$\|\mathbf{b}^h - A^h \mathbf{u}^{h,m}\|_\infty \leq 10^{-5} \cdot \|\mathbf{b}^h\|_\infty.$$

For the coarse grid problem, the domain is decomposed into  $M_x \times M_y$  subdomains. Unless otherwise indicated, ARTDI-DD iteration is carried out for the relative  $L^\infty$ -residual to become less than a per cent, with the artificial quality factor being 20.

Table 4 shows the number of  $V$ -cycles and CPU for the 3-grid algorithm, for various numbers of GS iterations ( $\gamma$ ). Set  $f = 10$  and  $q = 0$ ; choose  $h = 1/400$

Table 4: The number of  $V$ -cycles and CPU for the 3-grid algorithm, for various GS iterations. Set  $f = 10$  and  $q = 0$ ; choose  $h = 1/400$ ,  $h_c = 4h$ , and  $M_x \times M_y = 10 \times 1$ .

$\gamma$	$v = v_1$		$v = v_2$		$v = v_3$		$v = v_4$	
	$m$	CPU	$m$	CPU	$m$	CPU	$m$	CPU
1	11	11.8	11	11.5	11	12.6	11	12.7
2	6	7.2	6	7.8	6	7.5	6	7.0
3	5	6.5	5	6.8	5	6.7	5	6.3
4	4	5.5	5	7.3	4	5.5	5	6.8
5	4	6.0	4	6.1	4	6.0	5	7.6
10	4	7.9	4	8.1	4	8.1	5	9.9
100	3	33.9	7	78.7	3	34.2	diverge	

Table 5: The number of  $V$ -cycles for the 3-grid algorithm, for various grid size. Set  $f = 10$ ,  $q = 0$  ( $Q = \infty$ ), and  $M_x \times M_y = 16 \times 1$ . The coarse grid size  $h_c = 4h$ .

$1/h$	$v = v_1$	$v = v_2$	$v = v_3$	$v = v_4$
128	8	diverge	141	diverge
256	5	6	5	9
512	5	5	5	6
1024	5	5	5	6

and  $h_c = 4h$ . The coarse grid problem is decomposed into  $10 \times 1$  subdomains. The algorithm diverges for  $v = v_4$  when  $\gamma \geq 77$ . Note that the GS method decreases high-frequency components of the error, while it expands low-frequency components. As one can see from the table the 3-grid  $V$ -cycle converges best when  $\gamma = 3 \sim 5$ . (The similar has been observed when the coarse grid problem is solved directly.) Other experiences (not presented here) have shown that the 2-grid  $V$ -cycle performs best when  $\gamma = 3 \sim 4$ .

For the examples to be presented later in the section, we will choose  $\gamma = 3$ .

In Table 5, we present the number of  $V$ -cycles for the 3-grid algorithm, when  $f = 10$ ,  $q = 0$ , and the coarse grid size  $h_c = 4h$ . The coarse grid problem is decomposed into  $16 \times 1$  subdomains and solved up to the relative  $L^\infty$ -residual reduced by  $10^{-4}$ . The number of  $V$ -cycles seems independent of the mesh size  $h$  when the coarse grid problem is stable. When  $h = 1/128$ , the minimum grid frequencies (GFs) for the coarse grid problems are 6.4, 3.2, 5.1, and 3.3 for  $v_1$ ,  $v_2$ ,  $v_3$ , and  $v_4$ , respectively. (The average GFs are respectively 6.4, 6.7, 6.4, and 6.6.) The MG algorithm diverges

Table 6: The number of  $V$ -cycles and CPU for the 2-grid algorithm, for various frequencies. Set  $q = 0$ ,  $h = 1/512$ ,  $h_c = 2h$ , and  $M_x \times M_y = 16 \times 2$ .

$f$	$v = v_1$		$v = v_2$		$v = v_3$		$v = v_4$	
	$m$	CPU	$m$	CPU	$m$	CPU	$m$	CPU
5	5	57.5	5	56.0	5	56.6	5	76.7
10	5	48.1	5	50.2	5	53.6	5	57.0
20	5	43.6	5	43.3	5	43.7	5	52.0
40	7	57.8	18	181.6	9	77.3	diverge	

Table 7: The grid frequencies (GFs) for the coarse grid problem for  $f = 40$  in Table 6.

GF	$v = v_1$	$v = v_2$	$v = v_3$	$v = v_4$
minimum	12.8	6.4	10.2	6.4
average	12.8	13.2	13.0	13.5

for  $v_2$  and  $v_4$  and barely converges for  $v_3$ . It should be noticed that the MG iteration fails to converge due a lack of physical characteristics in the coarse grid solution; ARTDI-DD converges for the coarse grid problems for all cases. When  $h = 1/256$ , where GFs become twice those of the problem with  $h = 1/128$ , the convergence rates still deteriorate for  $v_2$  and  $v_4$ , due to local instability of the coarse grid problems.

Table 6 shows the number of  $V$ -cycles and CPU for the 2-grid algorithm, for various frequencies. Set  $q = 0$ ,  $h = 1/512$ , and  $h_c = 2h = 1/256$ . The coarse grid problem is decomposed into  $16 \times 2$  subdomains. When  $f \leq 20$ , the number of  $V$ -cycles ( $m$ ) is identically 5 for all different velocities and frequencies. In this frequency region, ARTDI-DD converges faster (and therefore CPU decreases) as the frequency increases; it is not clear to the authors what exactly causes this. For  $f = 40$ , the convergence rates deteriorate due to a certain degree of instability for the coarse grid problem. (Similar results were observed for higher accuracy solves for the coarse grid problems.) The minimum and average GFs for the coarse grid problems are given in Table 7. From Tables 6 and 7 and other various numerical experiments, we would like to conclude that the minimum GF should be at least 10-12 for stable solutions of high frequency waves.

In Table 8, we present the number of  $V$ -cycles and CPU for the 2-grid algorithm, for the frequency  $f = 50$  and for various physical quality factors  $Q$ . The artificial quality factor  $Q_a$  is set to be 20 for ARTDI-DD for the coarse grid problem, as in previous examples. Choose  $h = 1/1024$  and  $h_c = 2h$ . The coarse grid problem is

Table 8: The number of  $V$ -cycles and CPU for the 2-grid algorithm, for different quality factors  $Q$ . Choose  $f = 50$ ,  $h = 1/1024$ ,  $h_c = 2h$ , and  $M_x \times M_y = 32 \times 1$ .

$Q$	$v = v_1$		$v = v_4$	
	$m$	CPU	$m$	CPU
50	6	339	8	517
100	6	378	9	622
200	7	432	10	687
$\infty$	7	457	11	811

decomposed into  $32 \times 1$  subdomains. The number of iterations and the computation time increase as the medium becomes less attenuative; the convergence rate deteriorates more rapidly when the medium is heterogeneous. (The minimum GFs are 20.5 and 10.2 for  $v = v_1$  and  $v = v_4$ , respectively.)

## 6. Discussion

**The number of grid levels:** Since 20-40 grid points per wavelength are often enough for accurate solutions and one should choose at least 10-12 points per wavelength for stability reasons, it is reasonable to apply the MG method for 2-3 different grid levels. However, when a higher accuracy solution is to be computed, one can choose more grid levels to enjoy a fast computation of the MG algorithm as far as the coarsest grid problem captures characteristics of the physical problem.

**The smoothing operator:** The MG method can diverge for a large number of GS smoothing iterations, as shown in Table 4. One may adopt a smoothing operator which converges for an arbitrary number of iterations, such as CGNR (the conjugate gradient method applied to the normal equation).

**3D extension:** The most interesting and challenging task is to apply the MG algorithm and numerical findings to the simulation of high-frequency waves in 3D general media, utilizing high-performance parallel computers. We are pretty much interested in the subject [19].

**The relaxation parameter  $\beta$ :** Most of other DD methods have been studied for a constant medium ( $v \equiv 1$ ):  $K = 2\pi f$ . In the case, the relaxation parameter in (4.4) is chosen as  $\beta = K$ . However, it has been observed from various experiences that the DD iteration often fails to converge when either the grid frequency is not large enough or the domain is decomposed into a large number of subdomains including cross points. A better convergence can be achieved by choosing an appropriate complex-

valued relaxation parameter  $\beta(\mathbf{x})$ , defined on the subdomain interfaces, as suggested in [21]; we have adopted the complex-valued parameter for the results presented in this article.

**The artificial damping coefficient  $\eta$ :** The damping coefficient  $\eta$  in (4.13) has been found for ARTDI-DD to be most efficient when  $10 \leq G_f \leq 50$ . One may need to rectify it for different settings. A guideline is that the optimal damping coefficient grows ( $Q_a$  decreases) as the wave number and/or the number of subdomains increase. But the convergence rate deteriorates rapidly when  $Q_a \leq 10$  (over-damping).

**Local refinement:** One can consider mesh refinement near the sources, the discontinuities of the coefficients, and in lower velocity regions. In view to save computer storage and avoiding complicated data structures, it is natural to incorporate the *locally uniform mesh refinement* (LUMR) over subdomains where the strong variations are expected and retain coarser grids elsewhere. In the literature, LUMR has been studied for accurate and efficient solutions of transient problems [3, 35] and elliptic problems [6, 31]. DD methods provide a systematic and elegant way to implement LUMR. Certain engineering problems require high-frequency solutions of acoustic waves in a constant (or slowly-varying) background medium embedding lower velocity regions [23].

## 7. Conclusions

We have considered  $V$ -cycle multigrid (MG) methods for high-frequency numerical solutions of the Helmholtz problem. The grid frequency (GF) is defined to measure the number of grid points per wavelength. We have found from various numerical experiments that the minimum GF should be at least 10-12 for the coarse grid solution to capture characteristics of the physical problem. A nonoverlapping domain decomposition (DD) method has been adopted to solve the coarse grid problem that is still large for high-frequency solutions; an artificial damping iteration (ARTDI) is applied to accelerate the convergence of the DD method. It has been numerically verified that the coarse grid solver (ARTDI-DD) converges, independently on the mesh size and on the order of  $(M_x + M_y)$ , where  $M_x$  and  $M_y$  are the number of subdomains in  $x$ - and  $y$ -directions, respectively. The GS method is employed for the smoothing operator. The resulting MG method converges efficiently, independently on the mesh size and the wave number, when 3-5 GS iterations are applied for each of projections and prolongations and the coarse grid solution is stable; it may fail to converge when either the number of GS iterations is set too large or the coarse grid problem is not sufficiently fine. The MG method can be applied most practically with 2-3 grid levels.

## References

- [1] A. BAYLISS, C. GOLDSTEIN, AND E. TURKEL, *An iterative method for the Helmholtz equation*, J. Comput. Phys., 49 (1983), pp. 443–457.
- [2] —, *On accuracy conditions for the numerical computation of waves*, J. Comput. Phys., 59 (1985), pp. 396–404.
- [3] M. J. BERGER AND J. OLIGER, *Adaptive mesh refinement for hyperbolic partial differential equations*, J. Comput. Phys., 53 (1984), pp. 484–512.
- [4] T. BOURBIE, O. COUSSY, AND B. ZINSZNER, *Acoustics of porous media*, Institut francais du petrole publications, Gulf Publishing Company, Houston, London, Paris, Tokyo, 1987. Translated from the French by Nissim Marshall.
- [5] J. BRAMBLE, *Multigrid Methods*, Pitman Research Notes in Mathematics, Longman Scientific and Technical, Harlow, United Kingdom, 1993.
- [6] J. H. BRAMBLE, R. E. EWING, J. E. PASCIAK, AND A. H. SCHATZ, *A preconditioning technique for the efficient solution of problems with local grid refinement*, Comp. Meths. Appl. Mech. Eng., 67 (1988), pp. 149–159.
- [7] J. H. BRAMBLE, D. Y. KWAK, AND J. E. PASCIAK, *Uniform convergence of multigrid  $V$ -cycle iterations for indefinite and nonsymmetric problems*, SIAM J. Numer. Anal., 31 (1994), pp. 1746–1763.
- [8] J. H. BRAMBLE AND J. E. PASCIAK, *The analysis of smoothers for multigrid algorithms*, Math. Comp., 58 (1992), pp. 467–488.
- [9] X.-C. CAI, M. CASARIN, F. ELLIOTT, JR., AND O. WIDLUND, *Overlapping Schwarz algorithms for solving Helmholtz's equation*, in Domain Decomposition Methods 10, J. Mandel, C. Farhat, and X.-C. Cai, eds., vol. 218 of Contemporary Mathematics, Providence, RI, 1998, American Mathematical Society, pp. 391–399. Proceedings of the Tenth International Conference on Domain Decomposition Methods, August 10-14, 1997, Boulder, CO.
- [10] B. DESPRÉS, *Domain decomposition method and the Helmholtz problem*, in Mathematical and Numerical Aspects of Wave Propagation Phenomena, G. Cohen, L. Halpern, and P. Joly, eds., Philadelphia, 1991, SIAM, pp. 44–52.
- [11] —, *Domain decomposition method and the Helmholtz problem (part II)*, in Mathematical and Numerical Aspects of Wave Propagation, R. Kleinman, ed., Philadelphia, 1993, SIAM, pp. 197–206.

- [12] J. DOUGLAS, JR., J. L. HENSLEY, AND J. E. ROBERTS, *An alternating-direction iteration method for Helmholtz problems*, Appl. Math., 38 (1993), pp. 289–300.
- [13] M. DRYJA AND O. WIDLUND, *Some recent results on Schwarz type domain decomposition algorithms*, in Domain Decomposition Methods in Science and Engineering, A. Quarteroni, J. Periaux, Y. Kuznetsov, and O. Widlund, eds., vol. 157 of Contemporary Mathematics, Philadelphia, 1994, SIAM, pp. 53–61.
- [14] V. FABER AND T. MANTEUFFEL, *Necessary and sufficient conditions for the existence of a conjugate gradient method*, SIAM J. Numer. Anal., 21 (1984), pp. 352–362.
- [15] R. W. FREUND, *Conjugate gradient-type methods for linear systems with complex symmetric coefficient matrices*, SIAM J. Sci. Stat. Comput., 13 (1992), pp. 425–448.
- [16] W. HACKBUSCH, *Multigrid Methods and Applications*, Springer-Verlag, Berlin, 1985.
- [17] G. HOHMANN, *Numerical modeling for electromagnetic methods of Geophysics*, in Electromagnetic Methods in Applied Geophysics I: Theory, M. Nabighian, ed., Society of Exploration Geophysicists, Tulsa, Oklahoma, 1988.
- [18] W. JOUBERT AND D. YOUNG, *Necessary and sufficient conditions for the simplification of the generalized conjugate–gradient algorithms*, Linear Algebra Appl., 88/89 (1987), pp. 449–485.
- [19] S. KIM, *Numerical methods for the Helmholtz problem in 3D*. (in preparation).
- [20] —, *Parallel multidomain iterative algorithms for the Helmholtz wave equation*, Appl. Numer. Math., 17 (1995), pp. 411–429.
- [21] —, *Domain decomposition iterative procedures for solving scalar waves in the frequency domain*, Numer. Math., 79 (1998), pp. 231–259.
- [22] —, *On the use of rational iterations and domain decomposition methods for solving the Helmholtz problem*, Numer. Math., 79 (1998), pp. 529–552.
- [23] S. KIM AND S. KIM, *Frequency-domain numerical methods for acoustic waves in high-contrast media*. (in preparation).

- [24] S. KIM AND D. Y. KWAK, *Multigrid analysis for the Helmholtz wave equation*. (in preparation), 2001.
- [25] S. KIM AND M. LEE, *Artificial damping techniques for scalar waves in the frequency domain*, *Computers Math. Applic.*, 31, No. 8 (1996), pp. 1–12.
- [26] E. KJARTANSSON, *Constant Q-wave propagation and attenuation*, *J. Geophys. Res.*, 84 (1979), pp. 4737–4748.
- [27] P. LE TALLEC, *Domain decomposition methods in computational mechanics*, *Comput. Mech. Advances*, 1 (1994), pp. 121–220.
- [28] Q. LIAO AND G. MCMECHAN, *Multifrequency viscoacoustic modeling and inversion*, *Geophys.*, 61 (1996), pp. 1371–1378.
- [29] P. LIONS, *On the Schwarz alternating method III: a variant for nonoverlapping subdomains*, in *Domain Decomposition Methods for Partial Differential Equations*, T. Chan, R. Glowinski, J. Periaux, and O. Widlund, eds., Philadelphia, PA, 1990, SIAM, pp. 202–223.
- [30] S. MCCORMICK, *Multigrid Methods*, vol. 3 of *Frontiers in Applied Mathematics*, SIAM, Philadelphia, 1987.
- [31] S. MCCORMICK AND J. THOMAS, *The fast adaptive composite grid (FAC) method for elliptic equations*, *Math. Comp.*, 45 (1986), pp. 439–456.
- [32] L. MCINNES, R. SUSAN-RESIGA, D. KEYES, AND H. ATASSI, *Additive Schwarz methods with nonreflecting boundary conditions for the parallel computation of Helmholtz problems*, in *Domain Decomposition Methods 10*, J. Mandel, C. Farhat, and X.-C. Cai, eds., vol. 218 of *Contemporary Mathematics*, Providence, RI, 1998, American Mathematical Society, pp. 325–333. *Proceedings of the Tenth International Conference on Domain Decomposition Methods*, August 10-14, 1997, Boulder, CO.
- [33] Y. SAAD AND M. SCHULTZ, *GMRES: A generalized minimum residual algorithm for solving nonsymmetric linear systems*, *SIAM J. Sci. Stat. Comp.*, 7 (1986), pp. 856–869.
- [34] V. SHAIUROV AND E. OGORODNIKOV, *Some numerical methods of solving Helmholtz wave equation*, in *Mathematical and Numerical Aspects of Wave Propagation Phenomena*, G. Cohen, L. Halpern, and P. Joly, eds., Philadelphia, 1991, SIAM, pp. 73–79.

- [35] R. A. TROMPERT AND J. G. VERWER, *Analysis of the implicit Euler local uniform grid refinement method*, SIAM J. Sci. Comput., 14 (1993), pp. 259–278.
- [36] J. XU, *Iterative methods by space decomposition and subspace correction*, SIAM Review, 34 (1992), pp. 581–613.